ELSEVIER

Int. J. Therm. Sci. 41 (2002) 536–545

International Journal of Thermal Sciences

www.elsevier.com/locate/ijts

The BEM for point heat source estimation: application to multiple static sources and moving sources ☆

Frédéric Lefèvre *, Christophe Le Niliot

IUSTI, UMR CNRS 6595 Technopôle de Château Gombert, 5, Rue Enrico Fermi, 13453 Marseille cedex 13, France

Received 8 October 2001; accepted 7 March 2002

Abstract

This paper deals with an inverse problem, which consists of the identification of point heat sources in a homogeneous solid in transient heat conduction. The location and strength of the line heat sources are both unknown. For a single source we examine the case of a source which moves in the system during the experiment. The two-dimensional and three-dimensional linear heat conduction problems are considered here. The identification procedure is based on a boundary integral formulation using transient fundamental solutions. The discretized problem is non-linear if the location of the line heat sources is unknown. In order to solve the problem we use an iterative procedure to minimize a quadratic norm. The proposed numerical approach is applied to experimental 2D examples using measurements provided by an infrared scanner for surface temperatures and heat fluxes. A numerical example is presented for the 3D application.

Keywords: Inverse problem; Point heat source; Infrared thermography

1. Introduction

The inverse problem we propose to solve is the identification of the heat source term in the fundamental equation of heat transfer. In the present work, the considered heat source term is not a continuous function of space as proposed in [1], but a discontinuous set of point heat sources at unknown locations and of unknown strengths. This problem can have some interesting applications in various domains such as non-destructive control, for example the control of prestressed concrete bridge structure damaged by steel corrosion. The steel rods, heated by Joule effect can be assimilated to point heat sources in a 2D section. By filming the bridge with an infrared scanner, we obtain the superficial temperature and heat flux field on the bridge boundaries. The aim is to identify the heat dissipated by Joule effect in the steel rods and their location using superficial measurements only in order to estimate their corrosion level.

An other example is the identification of a fireball moving in a slag heap in order to prevent the blaze at the time when the fireball reaches the surface. In this case the fireball can be assimilated to a moving point heat source. The aim is to identify the path and the strength of the heat source using superficial measurements.

The other authors working on heat source identification propose methods such as the adjoint method [2] or the finite element method (FEM) [3]. In [4], Le Niliot has proposed the Boundary Element Method (BEM) for point heat sources strength identification in diffusive systems. In all these methods the location of the point heat sources must be known to solve the inverse problem of strength identification. Recently, Abou Khachfe [5] proposed the FEM associated to a conjugate gradient algorithm to cope with the location and strength identification of multiple point heat sources. This method has been tested on a 2D experiment and gives good results for the identification of two static sources. In [6], we have proposed the BEM to identify both the location and the strength of point heat sources in the steady case. This method tested on a 2D experiment gives good results for the identification of four sources.

In a recent work [7], we have proposed a BEM approach to identify the location and the strength of multiple heat

☆ This article is a follow up a communication presented by the authors at the EUROTHERM Seminar 68, "Inverse problems and experimental design in thermal and mechanical engineering", held in Poitiers in March 2001.

* Correspondence and reprints.

E-mail addresses: lefevre@genserver.insa-lyon.fr (F. Lefèvre), leniliot@iusti.univ-mrs.fr (C. Le Niliot).

1290-0729/02/$ – see front matter
PII: S1290-0729(02)01347-9

Nomenclature

$\boldsymbol{A}$	linear system matrix
B	second member vector
c	multiplying coefficient
D	diameter ..... m
$\boldsymbol{D}$	matrix of the first derivatives with respect to the coordinates
d	distance from the line heat source ..... m
g	heat source
Gr	Grashof's number
h	heat transfer coefficient ..... $W{\cdot}m^{-2}{\cdot}K^{-1}$
h_c	convective heat transfer coefficient $W{\cdot}m^{-2}{\cdot}K^{-1}$
$\boldsymbol{H}, \boldsymbol{G}$	matrices of BIE coefficients
$\boldsymbol{I}$	matrix for point source treatment
K	number of point sources
L	length of the bar ..... m
M	number of unknowns
N	number of boundary element
Nu_D	Nusselt's number for characteristic dimension D
P	heat flux vector
Pr	Prandtl's number
q^*	normal derivative of T^*
$\boldsymbol{Q}$	time regularization matrix
R	number of future time steps
S	source terms vector
s	space dimension ($s = 2$ in 2D and $s = 3$ in 3D)
t	time ..... s
T	temperature vector
T^*	fundamental solution
u	auxiliary variable
U	solution vector
x, y, z	Cartesian coordinates ..... m
X	coordinates vector

Greek symbols

η	time regularization parameter
δ	Dirac function
ε	emissivity
Γ	boundary of the diffusive domain
λ	conductivity ..... $W{\cdot}m^{-1}{\cdot}K^{-1}$
α	thermal diffusivity ..... $m^2{\cdot}s^{-1}$
φ	heat flux ..... $W{\cdot}m^{-2}$
θ	temperature in Celsius ..... °C
θ_0	initial temperature ..... °C
Θ	vector of the heat sources contribution
σ	standard deviation
Ω	diffusive domain
τ	time ..... s

Subscripts

k	point source index
∞	ambient conditions
r	radiative
c	convective

Superscripts

$\widehat{\ }$	least squares solution
$\sim$	approximated heat source contribution

Abbreviations

BEM	Boundary Element Method
FEM	Finite Element Method
BIE	Boundary Integral Equation
c.c.	curvilinear coordinates

sources in the transient case. This method can cope with the identification of the path and the strength of a single source moving in a diffusive domain. Compared to the FEM, the BEM does not require the complete mesh of the domain, but only the boundary mesh, which is particularly appropriated to the point heat source problem. Indeed, point source treatment with the BEM requires only the coordinates of the sources, without any refine domain mesh around the sources to cope with the high temperature gradient nearby these particular points.

In this paper, we present some experimental and numerical examples of the method described in [7]. Two different 2D experiments have been set up, one for the multiple static heat sources case and the other for the case of a single moving heat source. A numerical example is presented in the 3D case, which consists of the identification of the path and the strength of a moving heat source in a cone.

2. BEM for point heat source identification

In this part of the paper we describe the BEM approach for the point heat sources identification when both location and strength are unknown. The inverse method presented here is similar to our approach presented and detailed in [7] in the steady case. As it is pointed out in [4], the discretized boundary element equations are not linear when the source locations are unknown. An iterative method is proposed to minimize the distance between the modelled heat source contribution vector and the boundary variables contribution vector. The boundary variables can be given as a boundary condition or measured. We can also have some known internal temperatures. In our problem the number of sources is supposed to be known but, in some cases it is possible to find out the right number of the sources by examining the residuals (see [6]). In this section we describe the transient case formulation.

2.1. The boundary integral equation

Considering the point M, in a domain Ω of boundary Γ and integrating twice the linear fundamental heat transfer equation weighted by a fundamental solution T^* [8] lead to the Boundary Integral Equation (BIE) for the linear transient heat conduction:

$$c\theta_{M,t_F} + \int_{t_0}^{t_F}\int_{\Gamma} \alpha\theta q^* \,\mathrm{d}\Gamma\,\mathrm{d}t = \int_{t_0}^{t_F}\int_{\Gamma} \alpha\frac{\varphi}{\lambda}T^* \,\mathrm{d}\Gamma\,\mathrm{d}t + \int_{t_0}^{t_F}\int_{\Omega} \alpha\frac{g}{\lambda}T^* \,\mathrm{d}\Omega\,\mathrm{d}t + \int_{\Omega} \theta_0 T^* \,\mathrm{d}\Omega \tag{1}$$

Here φ is the heat flux, T^* the fundamental solution, q^* the normal derivative of T^* and c a coefficient which depends on the position of M. Namely, $c = 1$ if M is in Ω and $c < 1$ if M is on Γ (e.g., $c = 0.5$ if Γ is smooth at M).

The fundamental solution T^* is a time-and-space dependent function [9], which allows localised measurements (internal points) and singularities as point heat sources. The function T^* used to obtain Eq. (1) is a solution of:

$$\alpha\Delta T^* - \frac{\partial T^*}{\partial\tau} + \delta_M\delta_{\tau=0} = 0 \tag{2}$$

Here, δ_M and $\delta_{\tau=0}$ are the Dirac functions at point M and time τ, respectively and $\tau = t_F - t \cdot T^*$ represents the response to a point heat source in an infinite domain. Thus, T^* can be written:

$$T^* = \frac{1}{(4\pi\alpha\tau)^{s/2}}\exp\left(-\frac{d^2}{4\alpha\tau}\right)H(\tau) \tag{3}$$

Here, H is the Heaviside function, s is the space dimension and d is the distance from the considered point M to the current node of Γ. If the initial temperature field is uniform or stationary, the domain integral in Eq. (1) associated to the initial condition vanishes.

In the BIE (1) appears a volume integral relative to the heat source term g. In order to transform this volume integral in a discrete form without a complete domain mesh let us consider g as a set of K point heat sources. By applying the explicit form of T^*, the heat source term in BIE (1) can be written:

$$\int_{t_0}^{t_F}\int_{\Omega} \alpha\frac{g}{\lambda}T^* \,\mathrm{d}\Omega\,\mathrm{d}t = \sum_{k=1}^{K}\int_{t_0}^{t_F} \alpha\frac{g_k(t)}{\lambda}T^*_{i,k}\,\mathrm{d}t \tag{4}$$

Here, $g_k(t)$ is the algebraic strength of source k and $T^*_{i,k}$ is the fundamental solution given at Eq. (3) and calculated with $d_{i,k}$ the distance from the considered point M to the source k. As we can see in the latter equation, $T^*_{i,k}$ is then the response at point M to a strength variation of a point heat source k.

2.2. The heat source strength identification

It is important to notice that, as it is mentioned in [8], using (4) in (1) leads to a boundary integral formulation only. Thus a boundary discretisation is sufficient to solve the fundamental heat transfer equation.

As it is recommended by Brebbia et al. [8] and applied in [4], we use elements that are constant over space and linear over time. This last assumption means that the temperatures and heat flux are assumed to be constant on each element and linearly variable between two successive time steps. In a similar way, a linear variation in time for the heat source strength g_k within each time step will be assumed. The boundary Γ is discretized in N boundary nodes Γ_i. Introducing the coefficients $H_{i,j,F,f}$ and $G_{i,j,F,f}$ of the boundary integrals over an element Γ_j considering the boundary node on Γ_i we obtain the following equation:

$$\begin{aligned} c\theta_{i,F} + \sum_{f=1}^{F}\sum_{j=1}^{N}(H1_{i,j,F,f}\theta_{j,f-1} + H2_{i,j,F,f}\theta_{j,f}) &= \sum_{f=1}^{F}\sum_{j=1}^{N}(G1_{i,j,F,f}p_{j,f-1} + G2_{i,j,F,f}p_{j,f}) \\ &\quad + \sum_{f=1}^{F}\sum_{k=1}^{K}(I1_{i,k,F,f}g_{k,f-1} + I2_{i,k,F,f}g_{k,f}) \end{aligned} \tag{5}$$

Here $\theta_{j,f}$ is the temperature at element Γ_j at time t_f, $p_{j,f}$ is the heat flux at element Γ_j at time t_f, $I_{i,k,F,f}$ is the value of T^* considering node i, point source k and times t_F and t_f. The coefficients $H_{i,j,F,f}$ and $G_{i,j,F,f}$ can be found in [8]. $I_{i,k,F,f}$ is related to heat source coordinates.

Compared to the previous coefficients, the coefficient $I_{i,k,F,f}$ is not the result of a double integral on time and space but the value of a simple integral on time of the fundamental solution at node Γ_i considering the line source k. If the coordinates of the set of sources are known, it is possible to calculate these coefficients. Let introduce the auxiliary variable u_f given as:

$$u_f = \frac{d^2_{i,k}}{4\alpha\tau} \quad \text{with } \tau = t_F - t_f \tag{6}$$

where $d_{i,k}$ is the distance from the point heat source k to the boundary node Γ_i. Using the auxiliary variable u it is possible to integrate (4) analytically. As an example for the coefficient $I2_{i,k,F,f}$ we obtain:

$$\begin{aligned} I2_{i,k,F,f} &= \frac{t_F - t_{f-1}}{4\pi\,\Delta t_f}\left[\Gamma(0,u)\right]_{u_f}^{u_{f-1}} \\ &\quad - \frac{1}{4\pi\,\Delta t_f}\left[u\tau\,\Gamma(-1,u)\right]_{u_f}^{u_{f-1}} \end{aligned} \tag{7}$$

Here, $\Gamma(a,u)$ is the incomplete Gamma function [10] of the variable u and $\Delta t_f = t_f - t_{f-1}$. As we can see in Eqs. (6) and (7), the distance from the source k to boundary node Γ_i is included in some incomplete Gamma function of auxiliary

variable u. An initial guess is then necessary to use Eq. (5) for point heat source strength identification.

Considering the ill-posed character of the inverse problem for the strength identification procedure we use some future time steps as recommended by Beck et al. [11] and a Tikhonov's regularization procedure as recommended by Le Niliot [4].

The method of the future time steps consists in solving the problem at the resolution time t_F taking into account the measurements at times $t_F, t_{F+1}, \ldots, t_{F+R}$ in order to increase the sensitivity of the solution to the measurements at time t_F. Let us introduce the macro matrices $\boldsymbol{H}_{F,F+R}, \boldsymbol{G}_{F,F+R}$ that include the boundary equations at times t_{F+r} $(0 \leqslant r \leqslant R)$ and the macro matrix $\boldsymbol{I}_{F,F+R}$ that includes the coordinates of the point heat sources at times t_{F+r} $(0 \leqslant r \leqslant R)$. Let us introduce the matrix equations:

$$\boldsymbol{H}_{F,F+R}\begin{bmatrix} T_F \\ \vdots \\ T_{F+R} \end{bmatrix} = \boldsymbol{G}_{F,F+R}\begin{bmatrix} P_F \\ \vdots \\ P_{F+R} \end{bmatrix} + \boldsymbol{I}_{F,F+R}\begin{bmatrix} S_F \\ \vdots \\ S_{F+R} \end{bmatrix} + W_{F,F+R} \tag{8}$$

Here P_{F+r} (T_{F+r}) is a N-dimensional vector of the heat flux (temperatures) at the boundary at time t_{F+r} $(0 \leqslant r \leqslant R)$ and S_{F+r} is a K-dimensional vector of the heat source strength at time t_{F+r} $(0 \leqslant r \leqslant R)$. The macro matrices $\boldsymbol{H}_{F,F+R}$, $\boldsymbol{G}_{F,F+R}$ and $\boldsymbol{I}_{F,F+R}$ are triangular blocks whose elements are detailed in [4]. The vector $W_{F,F+R}$ contains all the information relative to the previous time steps $(t < t_F)$. Considering some unknown point heat sources at unknown locations, the system (8) is non-linear.

The system of Eq. (8) contains $N \times (R+1)$ equations and $(2 \times N + (s+1) \times K) \times (R+1)$ unknowns, namely $N \times (R+1)$ boundary temperatures, $N \times (R+1)$ boundary heat flux densities, $K \times (R+1)$ point heat source strengths and $K \times s \times (R+1)$ point heat sources coordinates, if we consider the possibility of moving sources in time. If we can find some boundary variables (at least one per element), which can be a prescribed temperature, a prescribed heat flux or both boundary variables prescribed, the number of unknown boundary variables at each time step can be reduced to $M \times (R+1)$.

Let us assume that the $K \times s \times (R+1)$ coordinates of the point heat sources are known as initially guessed locations or iteratively updated locations. As a result, the matrix $\boldsymbol{I}$ can be computed and the linear system (8) can be solved in the sense of vectors S_{F+r} $(0 \leqslant r \leqslant R)$ identification. Under all these assumptions it is possible to recast the system (8) into the linear system:

$$\boldsymbol{A}U = B \tag{9}$$

Here $\boldsymbol{A}$ is a matrix of dimension $(N \times (R+1), (M + K) \times (R+1))$, U is a vector of dimension $(M + K) \times (R+1)$ and B is a vector of dimension $N \times (R+1)$. In the general case we have more measurements than unknowns and U has to minimize a cost function $J(U)$. If we use a time regularization procedure (see [12]), the classical cost function is modified and U has to minimize functional $J(U)$ given by:

$$J(U) = \|\boldsymbol{A}U - B\|^2 + \eta\|\boldsymbol{Q}U\|^2 \tag{10}$$

Here $\boldsymbol{Q}$ is the time regularization matrix of dimension $((M + K) \times (R+1), (M + K) \times (R+1))$ and η is a regularization parameter. In all the following we will use a second order regularization. If we apply the least squares method to minimize the function (10), this leads to the vector $\widehat{U}$ as the solution of the square linear system of equations:

$$\left(\boldsymbol{A}^{\mathrm{T}}\boldsymbol{A} + \eta\boldsymbol{Q}^{\mathrm{T}}\boldsymbol{Q}\right)\widehat{U} = \boldsymbol{A}^{\mathrm{T}}B \tag{11}$$

Once the vector $\widehat{U}$ is obtained, we can determine the values of the estimated strengths $\hat{g}_k$ $(1 \leqslant k \leqslant K)$ and the boundary variables which are not prescribed at time t_{F+r} $(0 \leqslant r \leqslant R)$.

The approach presented in this part for point heat source strength identification is possible only if the coordinates of the sources are known in order to calculate the components of matrix $\boldsymbol{I}_{F,F+R}$. Contrary to the strength identification problem, the location identification problem is non-linear because the macro matrix $\boldsymbol{I}_{F,F+R}$ contains non-linear functions of the sources coordinates. Nevertheless, it is possible to calculate the first derivatives of this functions with respect to the coordinates. In this case we use an iterative method to identify the heat sources location. As the coordinates can be constant or function of time according to whether the sources are static or not, we have developed two different location identification procedures, one for the multiple static heat sources case and one for the single moving heat source case.

2.3. The location identification procedure for multiple static heat sources

The procedure for the multiple static heat sources case is not sequential but global, i.e., the coordinates are identified using the entire time steps, which gives a lot of information. Using the least squares approach it is possible to compare the space dependent heat source vector and the boundary measurements vector. Let us introduce two vectors $\widehat{\Theta}_f$ and $\widetilde{\Theta}_f$ $(0 \leqslant f \leqslant F)$, where:

$$\begin{bmatrix} \widehat{\Theta}_1 \\ \vdots \\ \widehat{\Theta}_F \end{bmatrix} = \boldsymbol{H}_{1,F}\begin{bmatrix} \widehat{T}_1 \\ \vdots \\ \widehat{T}_F \end{bmatrix} - \boldsymbol{G}_{1,F}\begin{bmatrix} \widehat{P}_1 \\ \vdots \\ \widehat{P}_F \end{bmatrix} \tag{12}$$

$$\begin{bmatrix} \widetilde{\Theta}_1 \\ \vdots \\ \widetilde{\Theta}_F \end{bmatrix} = \tilde{\boldsymbol{I}}_{1,F}\begin{bmatrix} \widehat{S}_1 \\ \vdots \\ \widehat{S}_F \end{bmatrix} \tag{13}$$

In the latter equations $\widehat{\ }$ denotes the least squares solution obtained from Eq. (11) at each time step and $\widetilde{\ }$ denotes the

heat sources location dependent vector. The vector $\widetilde{\Theta}_f$ is calculated using the iteratively updated, or initially guessed, locations contained in matrix $\tilde{\boldsymbol{I}}_{1,F}$ and the updated strengths contained in $\widehat{S}_f$.

In the inverse approach for heat sources location the aim is to minimize the distance between the vectors $\widehat{\Theta}_f$ and $\widetilde{\Theta}_f$ $(0 \leqslant f \leqslant F)$ and find out an estimate vector $\widehat{X}$ that contains the coordinates of the sources. As a result $\widehat{X}$ is solution of the following equation:

$$\widehat{X} = \arg\left\{ \min \left\| \begin{bmatrix} \widehat{\Theta}_1 \\ \vdots \\ \widehat{\Theta}_F \end{bmatrix} - \begin{bmatrix} \widetilde{\Theta}_1 \\ \vdots \\ \widetilde{\Theta}_F \end{bmatrix} \right\| \right\} \tag{14}$$

The proposed method can be decomposed into two steps; the first one consists of an identification of $\widehat{S}_f$, $\widehat{T}_f$ and $\widehat{P}_f$ at each time step t_f $(0 \leqslant f \leqslant F)$ using initially guessed or updated locations; the second one is a first order approximation of the matrix $\tilde{\boldsymbol{I}}_{1,F}$ with respect to the coordinates. The two steps are included in an iterative process. The employed method is a Newton method using the first term of the Taylor expansion of the fundamental solution contained in the matrix $\tilde{\boldsymbol{I}}_{1,F}$. Using a first order approximation leads to the linear system:

$$\begin{bmatrix} \widehat{\Theta}_1 \\ \vdots \\ \widehat{\Theta}_F \end{bmatrix} - \begin{bmatrix} \widetilde{\Theta}_1 \\ \vdots \\ \widetilde{\Theta}_F \end{bmatrix} = \boldsymbol{D}_{1,F} \Delta X \tag{15}$$

Here ΔX is a $(K \times s)$-dimensional vector of components Δx_k, Δy_k and Δz_k, the errors on source location k. The matrix $\boldsymbol{D}_{1,F}$ is a $(F \times N \times (K \times s))$-dimensional matrix consisting of the first derivatives of matrix $\boldsymbol{I}_{1,F}$ components with respect to the coordinates of the sources. An estimation $\Delta\widehat{X}$ of vector ΔX is obtained from system (15) by least squares. The new coordinates of the sources are updated to solve the inverse problem described by Eq. (11). If the number of sensors is sufficient the algorithm converges to the source locations with the correct strength. If during the iterative procedure a location is found outside the domain, a new location is randomly imposed within the domain.

Of course the initial guessed locations are very important in order to converge as rapidly as possible. In practical cases, these initial locations are chosen at the centre of the diffusive system but not at the same location in order to avoid a singular matrix $\boldsymbol{A}$.

The stopping criteria are based on coordinate variations between two iterations. Another stopping criterion could be introduced by calculating the norm $\|T_{\text{mes}} - \widehat{T}\|$, where the vector $\widehat{T}$ contains the calculated temperatures using the results of the inverse problem and a direct BEM approach. These calculated temperatures are compared to the vector of the measurements T_{mes}. The use of this criterion imposes the resolution of a direct problem at each iteration, which is not our aim.

2.4. The location identification procedure for a single moving heat source

The location identification procedure is similar to the one of the multiple static heat sources case. Nevertheless, we have to identify the coordinates of the source at each time step, which means that the iterative process occurs at each time step to identify both the strength and the location of the source. As for the strength identification procedure, we use the method of future time steps in order to increase the sensitivity of the solution to the measurements at time t_F. As the source is moving, the error on the location of the source is calculated for each future time step, which increases the number of unknowns. If we have R future time steps, the number of unknown locations is then equal to $s \times (R+1)$. For location identification, the aim is to find out a vector $\widehat{X}$ that contains the coordinates of the source at time steps t_{F+r} $(0 \leqslant r \leqslant R)$:

$$\widehat{X} = \arg\left\{ \min \left\| \begin{bmatrix} \widehat{\Theta}_F \\ \vdots \\ \widehat{\Theta}_{F+R} \end{bmatrix} - \begin{bmatrix} \widetilde{\Theta}_F \\ \vdots \\ \widetilde{\Theta}_{F+R} \end{bmatrix} \right\| \right\} \tag{16}$$

As in the multiple static heat sources case, the vectors $\widehat{\Theta}_{F+r}$ and $\widetilde{\Theta}_{F+r}$ are the solution of Eq. (11) resolution, but in this case we have to extract all the components $(\widehat{U}_F, \ldots, \widehat{U}_{F+R})$ of vector $\widehat{U}$ considering R future time steps. The errors Δx_k^{F+r}, Δy_k^{F+r} and Δz_k^{F+r} are calculated using a Newton method similar to the previous case. The new coordinates of the source are updated at each time step to solve the inverse problem described by Eq. (11). In order to reduce the sensitivity to measurements errors, we use the function specification method recommended by Beck et al. [11] in the strength identification procedure. We assume that the coordinates are constants over the R future time steps to identify the strength of the moving heat source.

3. Experimental 2D applications of point heat sources identification

In this section we propose two experimental identification examples based on the same 2D geometry. The experimental designs are two long square bars of section $50 \times 50\,\text{mm}^2$, one for the multiple static heat sources case and the other for the case of a single moving heat source. Each bar is crossed in its longest dimension by multiple thin KANTHAL® heating wires (diameter $\phi = 0.3$ mm and resistance $R = 29\,\Omega{\cdot}\text{m}^{-1}$), and this configuration represents a point heat source in a 2D section. The wires are heated by the Joule effect. The current is provided by some power supplies. As the system can be considered 2D at the centre of the bar, the heat source value is $g = V \times i/L$, where g is the strength in $\text{W}{\cdot}\text{m}^{-1}$, V is the measured voltage in Volts, i is the current in Amperes and L is the length of the bar (0.280 m).

The bar is fixed vertically on an optical bench. The infrared scanner is placed on the same bench. All the

surfaces are painted with a black paint of emissivity $\varepsilon = 0.95$ in the wavelength range of the scanner (8–12 μm). The proposed experimental set-up is very similar to the one proposed in [6].

In the presented examples, all the variables, i.e., heat flux and temperatures, are known along the square bar boundary, which is called the double specified boundary condition. The initial temperature field is equal to the ambiant temperature. The temperature measurements are obtained from an infrared AGEMA 880 Long Wave scanner. The infrared pictures constituted of 270×270 pixels (picture elements) are recorded on hard disc. In the obtained infrared picture used as a data-file it is necessary to extract 40 values, which represent 10 boundary elements over each side of the bar. To obtain this information from the picture we use a quadratic interpolation over the concerned pixels and the average temperature is then calculated at the middle of the element. The identified thermophysical properties of the bar are: $\lambda = 0.96\ \mathrm{W{\cdot}m^{-1}{\cdot}K^{-1}}$ and $\alpha = 5.3 \times 10^{-7}\ \mathrm{m^2{\cdot}s^{-1}}$.

The heat flux used as an extra boundary condition is obtained by associating the measured temperature field to a calculated non-linear heat transfer coefficient. Such restrictive boundary conditions are not essential to solve the inverse problem. The heat flux densities over the scanned surfaces are obtained as the sum of radiant and convective losses. For the radiant heat flux density we have: $\varphi_r = \varepsilon\sigma(T_\mathrm{r}^4 - T_i^4)$, where T_r is the radiant ambient temperature in Kelvin and T_i is the measured temperature at the element Γ_i of the scanned boundary in Kelvin. For the convective heat transfer coefficient $h_\mathrm{c}(t)$ we use the relation proposed by Elenbaas [13] for a short vertical cylinder in calm air. In the case of a cylinder of length L and diameter D we have:

$$Nu_D \exp\left(\frac{-2}{Nu_D}\right) = 0.6\left(Gr \cdot Pr \cdot \frac{D}{L}\right)_D^{1/4} \tag{17}$$

This correlation is used considering an average temperature along the studied section. Including radiant and convective losses, the measured heat flux density φ_i at boundary element Γ_i associated to the measured temperature θ_i is given by the relation:

$$\varphi_i(t, \theta_\infty, \theta_i, T_\mathrm{r}, T_i) = \varepsilon\sigma\left(T_\mathrm{r}^4 - T_i^4\right) + h_\mathrm{c}(t)(\theta_\infty - \theta_i) \tag{18}$$

Here ε is the emissivity. The ambient temperature θ_∞ in degree Celsius and the radiative temperature T_r in Kelvin are measured during the experiment. The radiative temperature is the temperature of the wall of a box surrounding the experimental apparatus and the ambient temperature is the temperature inside this box.

3.1. The static heat source case

The 2D section relative to the static heat source case is shown in Fig. 1. We have 4 different sources, from g_1 to g_4 situated in the four corners of the bar.

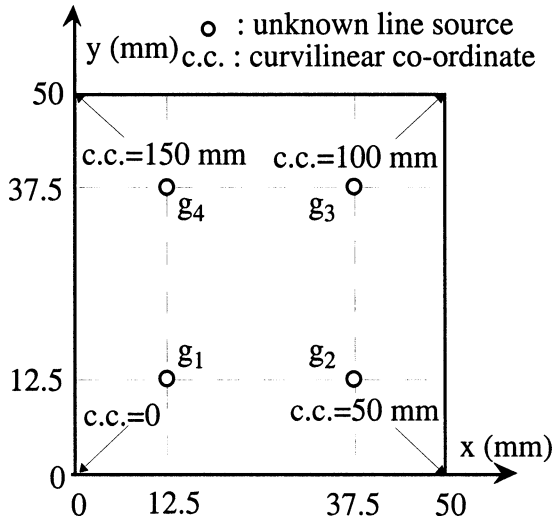

Fig. 1. The experimental section for the multiple static heat sources case.

Table 1
Identified coordinates

Source	Identified x, y		Coordinates errors		d (mm)
	x (mm)	y (mm)	Δx (mm)	Δy (mm)	
g_1	12.62	12.27	0.1	−0.2	0.3
g_2	36.70	13.31	−0.8	0.8	1.1
g_3	36.96	37.06	−0.5	−0.4	0.7
g_4	13.09	36.62	0.6	−0.9	1.1

The four sources are activated with different strength variations: $g_2(t)$ and $g_4(t)$ are sinusoidal and their phases are opposed, $g_1(t)$ is constant and $g_3(t)$ is triangular. The experiment lasted 3600 s and the time step used for the identification was $\Delta t = 36$ s. Six future time steps are used for the strength identification. The identified coordinates are given in Table 1. The distance d, given in mm, is the distance between the identified and the experimental source. As we can see from Table 1, the location is accurate with a maximum distance between the identified and the experimental source of 1.1 mm.

The identified strengths are displayed in Fig. 2. They are very satisfactory with an error less than 5% from the experimental strengths.

3.2. The moving heat source case

The 2D section relative to the moving heat source case is shown in Fig. 3. The moving point heat source is simulated by 15 heating wires activated successively. The experiment lasted 3600 s and the time step used for the identification is $\Delta t = 72$ s. In this case, four future time steps are sufficient to identify both the path and the strength of the point heat source, because the time step is twice as long as in the static heat source case. In this example, the moving heat source has an average speed of $78.5\ \mathrm{mm{\cdot}h^{-1}}$. Each heating wire is activated with a constant strength. The identified path in (x, y) diagram is given in Fig. 4(a) and the identified (x, y)

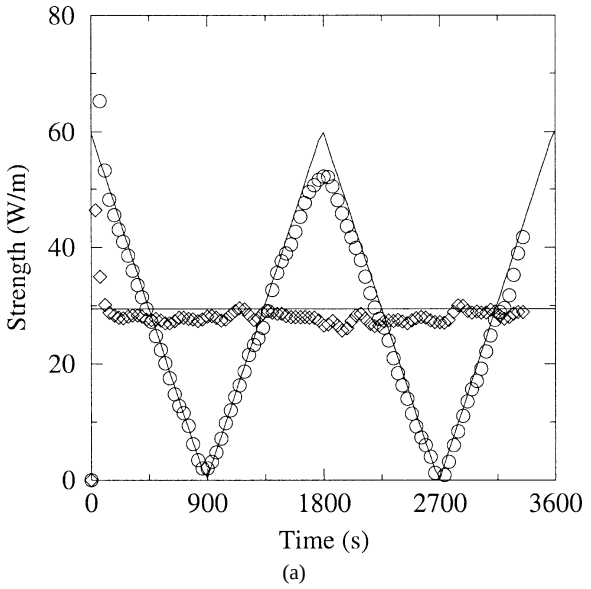

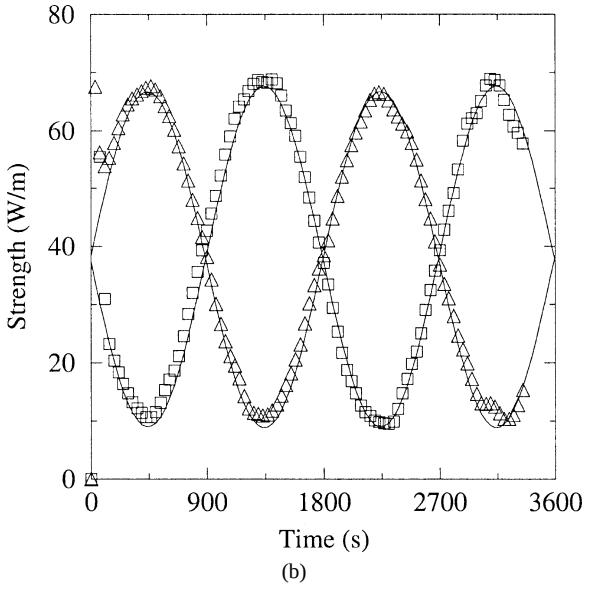

Fig. 2. Identified strengths ($W \cdot m^{-1}$) versus time (s) using the locations given in Table 1, $R = 6$, (a) g_1 (◇) and g_3 (◯), (b) g_2 (□) and g_4 (△), (— real strengths).

coordinates versus time are displayed in Fig. 4(b). As we can see, the identified locations at each time step are slightly dispersed around the real locations, which are steps.

In Fig. 5, we present the identified strengths at each time step. Compared to the multiple heat sources identification case, the identified strength is not smooth. The standard deviation between the real strength and the identified one is equal to $\sigma = 14.8\ W \cdot m^{-1}$, which is very important. This is due to the error in the location identification. Nevertheless, the average of the difference between the real strength and the identified strength at all the time steps is about $6.4\ W \cdot m^{-1}$, which shows that the global energy is well recovered.

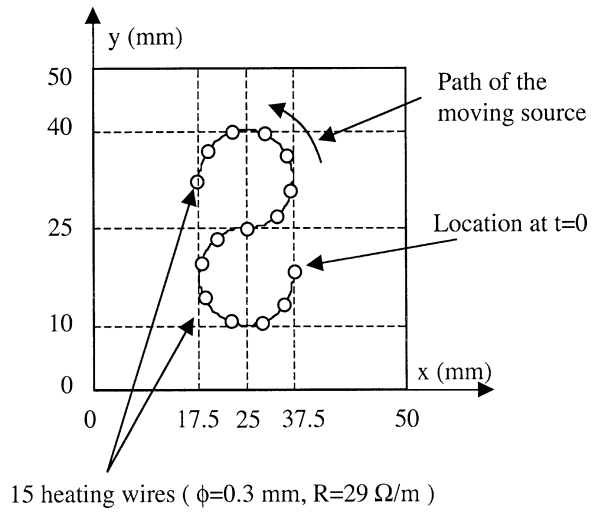

Fig. 3. The experimental section for the moving heat source.

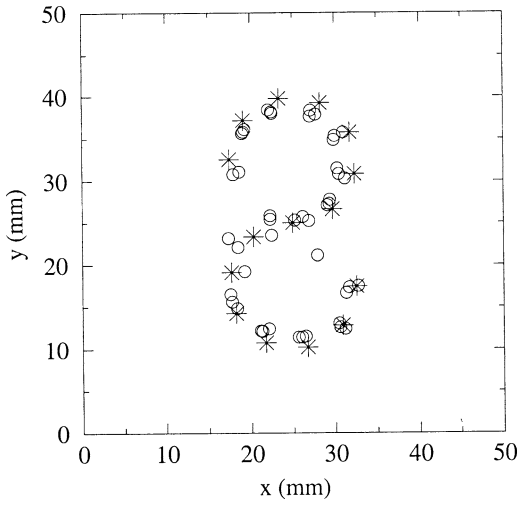

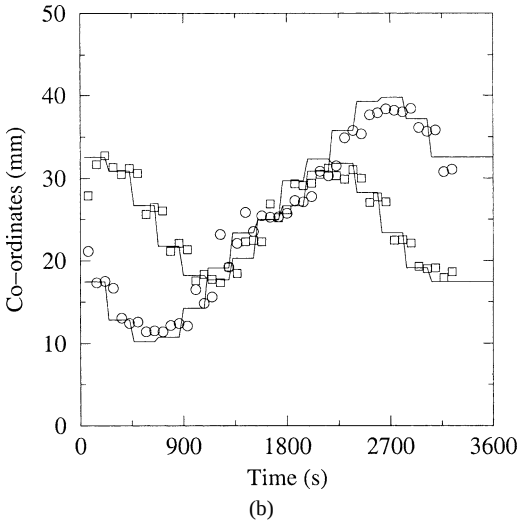

Fig. 4. (a) Identified locations (◯) of a moving source at each time step, $R = 4$, (∗ real location), (b) Identified coordinates x (□) and y (◯), (— real values).

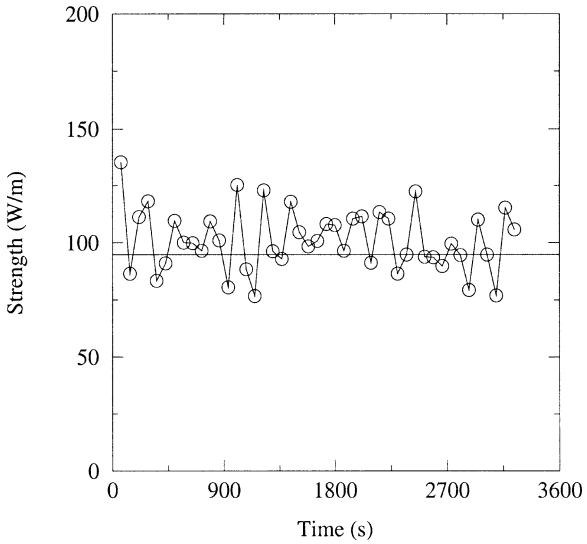

Fig. 5. Strength identification using the identified locations at each time step, $R = 4$.

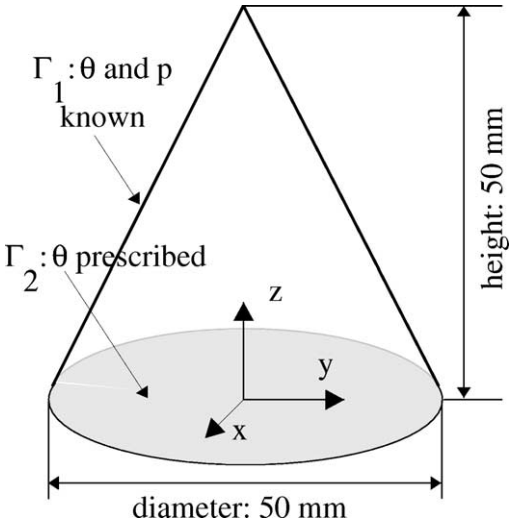

Fig. 6. Scheme of the 3D diffusive system, dimensions and boundary conditions.

4. A 3d numerical example of a single moving source

The 3D example is treated here in order to show the capabilities of the numerical method described previously. The diffusive system proposed here is a reduced model of a slag heap. It is a 50 mm height cone with a base of 50 mm diameter (see Fig. 6) and the thermal properties used are nearly those of cement ($\lambda = 1$ W·m^{-1}·K^{-1}, $\alpha = 0.5 \times 10^{-6}$ m^2·s^{-1}).

The only example presented is a single moving source of triangular strength describing a helical path within the cone from the top to its base (see Fig. 7). The boundary mesh is composed of 16 triangular and 48 square elements on the cone (Γ_1) and 16 triangular and 24 square elements on the circular base (Γ_2).

The experiment is performed during 3600 s with 50 time steps. For this example all the boundary conditions are known. A linear heat losses coefficient $h = 10$ W·m^{-2}·K^{-1} is applied on the cone boundary (Γ_1) when the base (Γ_2) is kept at zero degree ($\theta(x, y, 0, 0) = 0\,^\circ$C). A homogeneous temperature $\theta(x, y, z, 0) = 0\,^\circ$C is taken as the initial condition. For the inverse application, the boundary Γ_1 is scanned and both the temperature and the heat flux are assumed to be measured. The temperature on Γ_2 is given as a Dirichlet boundary condition and is assumed to be exact.

In order to take into account some measurement errors, the numerical data are disrupted by an additional normal error of zero mean value and standard deviation $\sigma = 0.5\,^\circ$C. Such a formulation leads to random errors at 99% reliance in the range $[-2.576\sigma; 2.576\sigma]$. The random numbers are generated by the routine RAN1 of [14].

The data produced by the direct numerical simulation and disrupted by a Gaussian noise ($\sigma = 0.5\,^\circ$C) is used to solve the inverse problem. In this example the location given to initialize the iterative process at the beginning of the sequential procedure of strength and location estimation

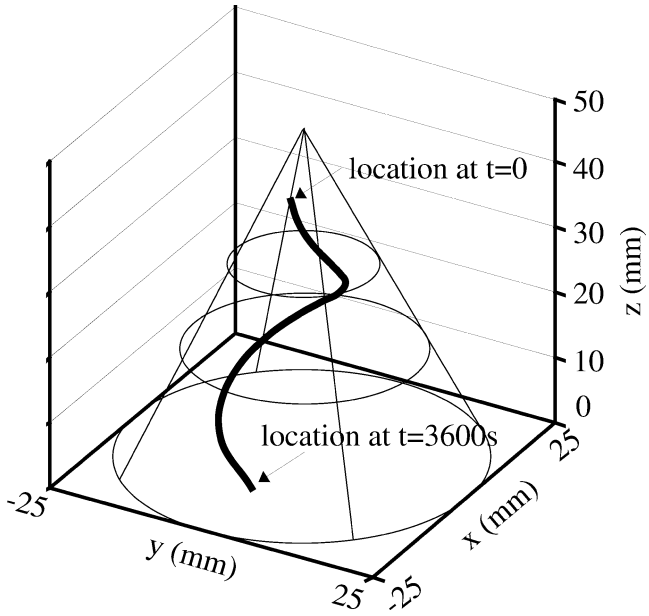

Fig. 7. Path followed by the point heat source in the 3D system during 50 time steps of 72 s.

is $x = y = 0$ and $z = 25$ mm. The identified path is given in Fig. 8(a) in (x, z) diagram and in Fig. 8(b) in (x, y) diagram. As we can see, the path is well recovered except for the base of the cone where there is a lack of information. As we can see, the method can cope with 3D cases provided that the strength of the moving source is sufficient to have non-zero sensitivity to location and strength, and that the Fourier number is high enough to solve the inverse problem. In the presented examples these conditions are verified. In Fig. 9, we present the result of the strength identification.

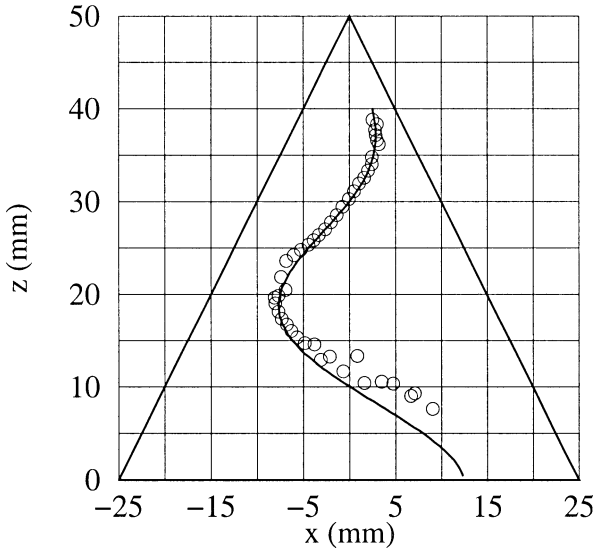

(a)

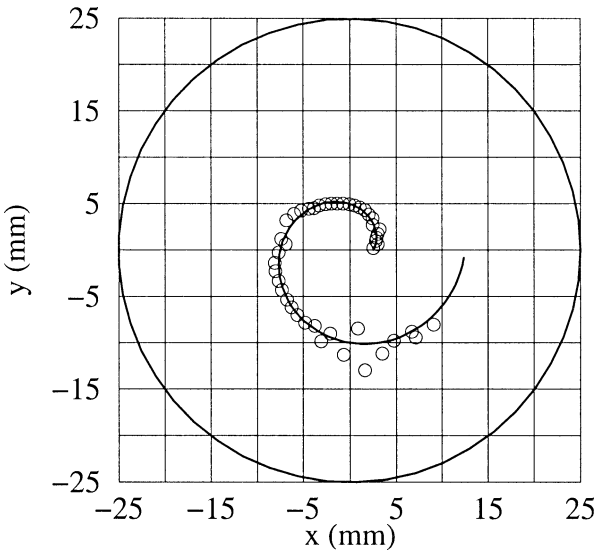

(b)

Fig. 8. Results of identification of a moving source in a 3D system, $\sigma = 0.5\,^{\circ}\mathrm{C}$, (a) identified path projection on plane $x-z$, (b) identified path projection on plane $x-y$.

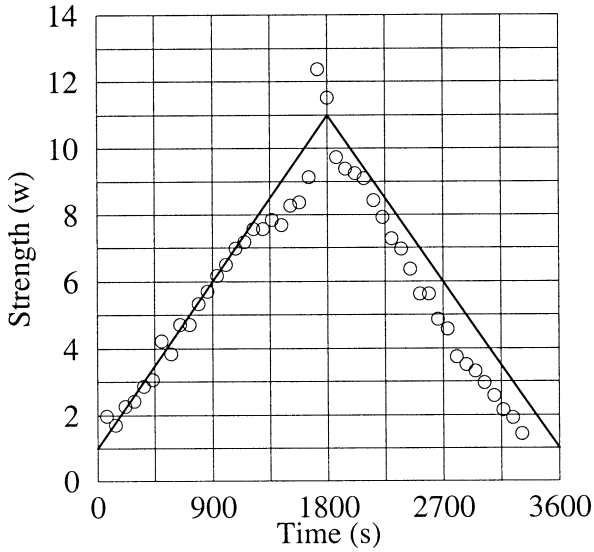

Fig. 9. Strength identification using the identified locations at each time step, $R = 4$, $\sigma = 0.5\,^{\circ}\mathrm{C}$.

5. Conclusion

In this paper we have presented our approach for multiple point heat sources identification in the transient case. This method is based on a Boundary Element Method formulation, which is well adapted to the point heat source identification problem. Indeed, taking into account point heat sources with the BEM does not require any refine domain mesh around the point sources, but only a boundary mesh and the calculation of incomplete Gama functions, which depend on the sources coordinates. This property makes the BEM more adapted to the problem of point sources identification than other classical numerical methods, such as the finite element method, for which point heat sources are mathematical singularities. Nevertheless, the boundary element method is restricted to linear problems in the transient case.

The identification method, developed in this paper, permits to identify both moving and static sources. The results of the method combining the location and strength identification are satisfactory considering the 2D experimental examples. They show that a set of point heat sources can be identified using surface measurements only. Compare to the other methods, described in the literature, our method permits to identify more than 2 sources and can be applied to moving heat sources.

An experiment has been set up to simulate a moving point heat source using multiple heating wires activated successively. The results show that it is possible to identify both the path and the strength of a source moving in a 2D diffusive system. A numerical 3D example has been presented to show the capabilities of the method. In this last case the main difficulty is to produce an experimental point source with a sufficient strength to permit the reconstruction of the path covered by the source. An application of this 3D case could be the identification of a fireball moving in a slag heap in order to prevent the blaze at the time when the fireball reaches the surface.

References

[1] T.J. Martin, G.S. Dulikravich, Inverse determination of boundary conditions and sources in steady heat conduction with heat generation, J. Heat Transfer 118 (1996) 546–554.

[2] A.J. Silva Neto, M.N. Ozisik, Two-dimensional inverse heat conduction problem of estimating the time-varying strength of a line heat source, J. Appl. Phys. 71 (1992) 5357–5362.

[3] C. Yang, The determination of two heat sources in an inverse heat conduction problem, Internat. J. Heat Mass Transfer 42 (1999) 345–356.

[4] C. Le Niliot, The boundary element method for the time varying strength estimation of point heat sources: Application to a two-dimensional diffusion system, Numer. Heat Transfer B 33 (1998) 301–321.
[5] R. Abou Khachfe, Résolution numérique de problèmes inverses 2D non linéaires de conduction de la chaleur par la méthode des éléments finis et l'algorithme du gradient conjugué-Validation expérimentale, Ph.D. Thesis, Ecole polytechnique de Nantes, France, 2000.
[6] C. Le Niliot, F. Lefèvre, A method for multiple steady line heat sources identification in a diffusive system: Application to an experimental 2D problem, Internat. J. Heat Mass Transfer 44 (2001) 1425–1438.
[7] C. Le Niliot, F. Lefèvre, Multiple transient point heat sources identification in heat diffusion: Application to numerical 2d and 3d problems, Numer. Heat Transfer B 39 (2001) 277–301.
[8] C.A. Brebbia, J.C.F. Telles, L.C. Wrobel, Boundary Element Techniques, Springer-Verlag, Berlin, 1984.
[9] M.N. Ozisik, Heat Conduction, 2nd edn., Wiley, New York, 1993.
[10] M. Abramowitz, I.A. Stegun, Handbook of Mathematical Functions, Dover, New York, 1972.
[11] J.V. Beck, B. Blackwell, C.R. St. Clair, Inverse Heat Conduction, Ill-Posed Problems, Wiley–Interscience, New York, 1985.
[12] A.N. Tikhonov, V.Y. Arsenin, Solutions of Ill-Posed Problems, Winston and Sons, Washington, DC, 1977.
[13] W. Elenbaas, The dissipation of heat by free convection from vertical and horizontal cylinders, J. Appl. Phys. 19 (1948) 1148–1154.
[14] W.H. Press, B.P. Flannery, S.A. Teulossky, W.T. Vetterling, Numerical Recipes, Cambridge University Press, Cambridge, 1990.